

Direct Observation of Momentum-Dependent Local-Field Effects in Solid Nitrogen

C. Tarrío and S. E. Schnatterly

Jesse Beams Laboratory of Physics, University of Virginia, Charlottesville, Virginia 22901

(Received 12 November 1990)

We have measured the momentum dependence of the $a^1\Pi_g \leftarrow X^1\Sigma_g^+$ transition in cubic solid nitrogen. We have evaluated the oscillator strength of the transition and compared it to the markedly different strength found in analogous measurements on the gas, and conclude that local-field effects present in the solid are responsible for the differences found. This is the first momentum-dependent measurement of local fields in a solid. The local-field enhancement factor increases by about a factor of 3 over the momentum range covered, and is consistent with a simple model calculation for small momenta.

PACS numbers: 78.20.Bh, 79.20.-m

Local-field effects are an important subject in the study of electronic properties of solids. In the presence of an external electric field, the microscopic field experienced by an atom or point defect in a solid is enhanced due to dipole moments induced on the surrounding atoms. In the simplest model, that of point dipoles on a cubic lattice at zero wave vector, this field is given by the Clausius-Mossotti relation.¹ In solids in which the electric field is spatially varying, this result is no longer valid. Thus the wave-vector dependence of local fields must be known in order to understand the electronic properties of systems with nanostructures, interfaces, or interacting point defects. In this Letter we report the first measurements of local-field strengths in a solid for finite wave vectors.

To observe local fields in solids, the electronic states used as a probe must be highly localized. Solid gases, in which the only interactions between neighboring atoms or molecules is the van der Waals interaction, can provide good test systems. In the rare-gas solids the Clausius-Mossotti relation has been shown to give accurate values for the optical dielectric constant based on atomic polarizability data.²

Cubic solid nitrogen has been shown to have electronic transitions similar to those in the free molecule.³⁻⁵ In particular, the Lyman-Birge-Hopfield (LBH) transition, $a^1\Pi_g \leftarrow X^1\Sigma_g^+$, centered around 9.1 eV, has been measured, revealing structure similar to that of the free molecule.^{4,5} This transition is dipole forbidden, quadrupole allowed in both the gas and the solid. In a simple model the strength of a quadrupole transition would be expected to grow quadratically with momentum. The momentum dependence of the LBH transition has been studied in the gas,⁶⁻⁸ and a quadratic increase in the cross section was observed for small momenta.

Nagel and Witten⁹ have predicted that local fields in solids vary with wave vector throughout the Brillouin zone. To observe this effect, a transition must be found which is isolated in energy from other absorption. The strength of the transition must be measured as a function

of momentum transfer in both the solid and gas phases. We have measured the momentum dependence of the LBH transition in the cubic solid phase and compared our results to those obtained on the gas.⁶⁻⁸ We discuss the difference between the two cases in light of the model of Nagel and Witten.⁹

In the zero-momentum limit, the dielectric constant of a solid can be related to the molecular polarizability by the Clausius-Mossotti or Lorentz-Lorenz relation:¹

$$\epsilon(\omega) = 1 + \frac{4\pi n\alpha(\omega)}{1 - (4\pi/3)n\alpha(\omega)}, \quad (1)$$

where $\epsilon = \epsilon_1 + i\epsilon_2$ is the complex dielectric function of the solid, $\alpha = \alpha_1 + i\alpha_2$ is the complex molecular polarizability, and n is the molecular density of the solid. In this expression the factor $1/[1 - (4\pi/3)n\alpha]$ is a local-field correction due to the dipole moments induced on atoms surrounding the excited one. In the gas-phase measurements of Ref. 6, the molecular densities, on the order of 10^{13} cm^{-3} , lead to local-field enhancements on the order of 10^{-10} . Nagel and Witten⁹ have developed a momentum-dependent model to take into account the different local fields present in different parts of the Brillouin zone of a solid. They rewrite Eq. (1) as

$$\epsilon(q, \omega) = 1 + \frac{4\pi n\alpha(\omega)}{1 - B(q)n\alpha(\omega)}, \quad (2)$$

where q is the momentum transfer and $B(q)$ is the local-field factor which is a measure of the enhancement of the local field relative to the macroscopic field in the solid. They have evaluated $B(q)$ in the point-dipole approximation for the three principal axes of the three cubic structures. In the zero- q limit $B(q)$ approaches the Lorentz-Lorenz value of $4\pi/3$. To compare cross sections between the solid and gas phases, we evaluate the imaginary part of Eq. (2):

$$\epsilon_2(q, \omega) = \frac{4\pi n\alpha_2(q, \omega)}{[1 - B(q)n\alpha_1(q, \omega)]^2}. \quad (3)$$

Here we have used the approximation $B(q)n\alpha_2(\omega) \ll 1$,

which is accurate in the momentum and energy ranges we have covered. We have also allowed the molecular polarizability to vary with both energy and momentum.

Thus, if we have data on the molecular polarizability and the solid-state dielectric function, we can directly evaluate $B(q)$. Several groups have measured the gas-phase momentum-dependent cross section for the LBH transition,⁶⁻⁸ which is proportional to the imaginary part of the polarizability,¹⁰ with good agreement among the results. We have measured the solid-state cross section, which is proportional to $\text{Im}(-1/\epsilon(q,\omega))$,¹¹ as a function of momentum. From a Kramers-Kronig analysis, we can find $\epsilon(q,\omega)$, and thus evaluate $B(q)$. The data reported by gas-phase spectroscopists are in terms of the generalized oscillator strength $f(q)$, which is a measure of the effective number of electrons participating in the transition. From our data we evaluate the solid-state oscillator strength $N_{\text{eff}}(q)$ from

$$N_{\text{eff}}(q) = \frac{2}{\pi\omega_p^2} \int_{\omega_{\text{min}}}^{\omega_{\text{max}}} \epsilon_2(q,\omega')\omega' d\omega', \quad (4)$$

where the integral is over the energy range of the transition and ω_p is an effective plasma frequency assuming one electron per molecule. Equation (3) can then be expressed in terms of the oscillator strengths as

$$B(q) = \frac{1}{na_1(q,\omega_1)} \left[1 - \left(\frac{f(q)}{N_{\text{eff}}(q)} \right)^{1/2} \right], \quad (5)$$

where ω_1 is the energy of the transition, about 9.1 eV. We evaluate $a_1(q,\omega_1)$ from our values of $\epsilon_1(q,\omega_1)$.

Measurements were made on the University of Virginia IES accelerator, which is described in Ref. 12. They were made possible by a new low-temperature sample mount described in Ref. 13. Gas was allowed into the sample chamber through a needle valve and flowed over substrates held at about 30 K. The deposition parameters were varied. Flow rates led to pressures between 3×10^{-6} and 3×10^{-5} Torr and deposition times varied between 30 s and 6 min. Resulting films were estimated to be between 300 and 1000 Å thick. The background pressure was $< 10^{-8}$ Torr with the sample mount warm and $< 10^{-9}$ Torr with the sample mount cold. Electron-diffraction patterns revealed a polycrystalline cubic structure with $a_0 = 5.65 \pm 0.02$ Å. Wyckoff¹⁴ reports the α phase of N_2 , stable below 35 K, having a fcc structure with $a_0 = 5.644$ Å. Samples were deposited onto the following substrates: 100 Å carbon, 300 Å aluminum, and 700 Å MgF_2 .

The primary beam energy was 285 keV, with energy resolution between 70 and 120 meV during the measurements. Momentum resolution was about 0.06 \AA^{-1} during the measurements. An energy range of 2 to 60 eV was measured for each value of momentum. Momentum transfers between 0.1 and 1.1 \AA^{-1} were measured. The lower-momentum limit is due to kinematic factors and

resolution, while the upper limit is due to increasing thermal diffuse scattering, in which a fast electron scatters quasielastically from a phonon, and inelastically at low wave vector from an electronic excitation, as well as increasing uncertainties in the multiple-scattering correction and the decreasing cross section.

Measured spectra contain contributions from both the sample and the substrate. Substrate spectra were measured separately at the same momentum transfer and temperature for each corresponding N_2 spectrum. In all cases a spectrum was measured from 2 to 60 eV for samples deposited on carbon. Low-energy (2–12 eV), high-resolution spectra were measured for samples deposited on either C or Al, with a few spectra measured on MgF_2 . Substrate spectra were also measured to examine the possibility of residual gases in the sample chamber plating out and contaminating the samples. After the substrates had been cold for about 10 days, some contamination was observed. To prevent this, the sample mount was allowed to warm up every few days and a fresh sample film was prepared.

To obtain the N_2 spectra, the substrate spectra were subtracted from the total spectra at the corresponding q values. Substrate spectra were scaled to the total spectra from 2 to 7 eV, well below the absorption threshold, and the estimated contributions were subtracted from the total spectra. C spectra contributed about 5%–20% of the total at the carbon plasmon (24 eV), the most intense feature of the C spectrum. The contribution was a much larger fraction at the LBH transition, especially at low q . For this region, low-energy spectra were also measured on Al substrates, which have much weaker absorption at these energies. No measurable differences were observed in the results using the different substrates.

To obtain the energy-loss function $\text{Im}(-1/\epsilon)$ we use algorithms of Fields¹⁵ and of Livins, Aton, and Schnatterly.¹⁶ The final scale of the spectrum is determined by satisfying constraints on the oscillator-strength sum rule, assuming 10.5 electrons and the low-frequency dielectric constant, which is discussed below. A value slightly higher than the 10 electrons occupying the outer orbitals was assumed because outer-shell electrons tend to carry more than their share of the total oscillator strength.¹⁷ Resulting energy-loss functions for a variety of momentum transfers are shown in Fig. 1. The low- q energy-loss function and dielectric constants agree well with those measured by Daniels.³ As can be seen, the LBH transition, centered around 9.1 eV, clearly grows in amplitude with increasing q .

We are able to resolve at least eight vibrational states in the LBH transition for $q > 0.3 \text{ \AA}^{-1}$. Because of the presence of weak magnetic dipole transitions in the vicinity of the higher vibrational states of the LBH series, we have used a fitting procedure to evaluate the oscillator strengths. We assumed a constant separation between peaks and fit Gaussians to the first seven peaks of the

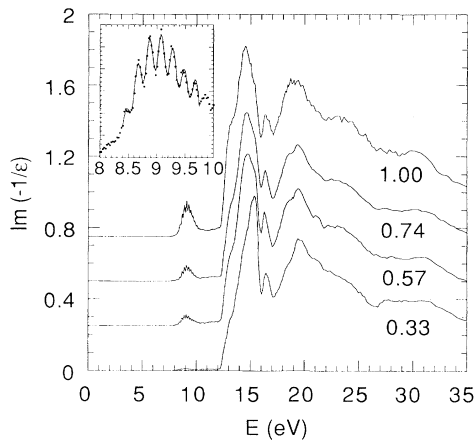


FIG. 1. $\text{Im}(-1/\epsilon)$ of $\alpha\text{-N}_2$ obtained at four values of momentum transfer. Labels below the curves indicate the momentum transfer in \AA^{-1} .

series. The Gaussian shape accounts for both our energy resolution and thermal broadening. Reduced χ^2 obtained from the fits ranged from 1.5 to 4. One such fit is shown in the inset in Fig. 1. To find the total strength we assumed a Poisson distribution for the entire series, and evaluated the strengths based on the contribution from the three most intense peaks. To check the validity of this procedure, we also evaluated the strength directly from 8.2 to 9.8 eV in the spectra. There was more scatter in the values obtained in this manner, but the results generally agreed, especially for $q > 0.6 \text{ \AA}^{-1}$. To compare our data to those obtained on the N_2 molecule, we have digitized the data of Skerbele and Lassette.⁶

Figure 2 shows the resulting molecular and solid-state oscillator strengths. The solid-state strength is greater at every value of momentum transfer. Some of this added intensity is due to the presence of odd-parity phonons, which mix some dipole character into the transitions. The expansion of the transition matrix element then consists of the quadrupole element, the phonon mixing element, which is momentum independent, and cross terms which average to zero. Thus, we have subtracted a constant value from our oscillator strength for further comparison with the gas-phase data. More important than the greater strength, however, is the different functional dependence. The free-molecule results begin to increase quadratically at low momentum, then increase more gradually above 0.6 \AA^{-1} .⁶ On the other hand, the solid-state strength increases more rapidly at higher momenta. If the local-field effects were constant with momentum transfer, we would expect about a 6% increase in strength going from the gas to the solid over the entire momentum range covered.

In order to be self-consistent, we have used an iterative procedure to obtain $B(q)$. In Eq. (5) both $N_{\text{eff}}(q)$ and $\alpha_1(q, \omega_1)$ are dependent on our choice of the low-

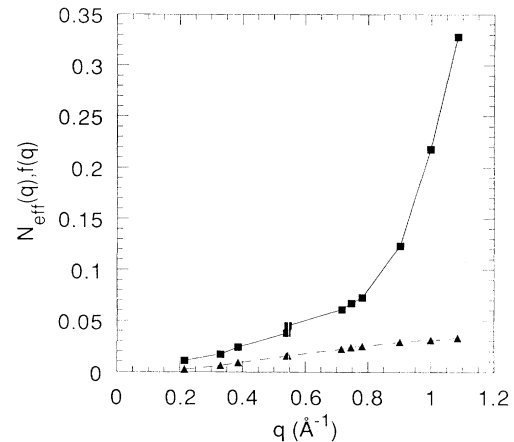


FIG. 2. Oscillator strength of the LBH transition measured in the gas phase (triangles with dashed line, from Ref. 6) and the cubic solid phase (squares with solid line).

frequency dielectric constant via the Kramers-Kronig analysis. Therefore, for each spectrum we have assumed an input value of $B(q)$ and determined a low-frequency dielectric constant using Eq. (2) and the molecular polarizability in Ref. 18. From the dielectric function and $N_{\text{eff}}(q)$, we then determine an output value for $B(q)$ and compare the result to the input value. This procedure is then iterated until the input and output values were within 0.5% of one another. A difference of 5% in the input value of $B(q)$ made a difference of (2-3)% in the output value in most cases.

Figure 3 shows the results we have obtained using this procedure. We have subtracted odd-parity phonon contributions to N_{eff} assuming that $B(q)$ must extrapolate to the Lorentz-Lorenz value of $4\pi/3$ at $q=0$, which is

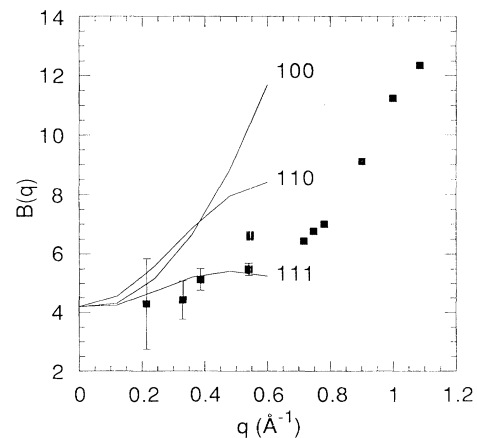


FIG. 3. Local-field factor $B(q)$. Solid lines, from Ref. 9, with labels indicating the principal crystal axes; squares, calculated as described in text. Error bars represent the uncertainty due to odd-parity phonon oscillator-strength subtraction.

known to be accurate for cubic solid gases.² For comparison, we show $B(q)$ calculated by Nagel and Witten⁹ for the three principal axes of the fcc structure. The calculations were performed up to $q = \pi/a = 0.56 \text{ \AA}^{-1}$. At low q it is evident that our results are quite sensitive to the oscillator-strength subtraction, and the uncertainty due to the substrate subtraction is also quite large. Our results do, however, fall in the neighborhood of the calculated $B(q)$, and seem to favor the result for the [111] direction. In the high- q range, where there are no calculations, the results are not sensitive to the strength subtraction, although thermal diffuse scattering may add uncertainty in the high- q range. It is apparent that $B(q)$ increases sharply in the range $0.6 < q < 1.1 \text{ \AA}^{-1}$. $B(q)$ cannot continue to increase indefinitely. If $B(q)$ continues to grow, the denominator in Eq. (3) will eventually approach zero, resulting in a lattice instability. Thus, $B(q)$ must reach a maximum value less than 19 and approach zero in the limit of infinite momentum due to the finite size of the N_2 molecule. Inelastic-x-ray scattering may be a feasible way to probe the behavior of $B(q)$ for very-large- q values.

In summary, we have reported the first direct observation of momentum-dependent local-field effects in a solid material. Our evaluation of the local-field factor is consistent with theoretical predictions for small q . The sharp increase in the local-field factor for large wave vectors indicates that local fields are very important in systems with spatially varying electric fields.

Research supported in part by NSF Grant No. DMR-88-19052. We would like to thank D. Metcalf for manuscript suggestions and other members of our group, D. Carson, D. Husk, S. Velasquez, and E. Benitez, for

helpful discussions.

¹J. D. Jackson, *Classical Electrodynamics* (Wiley, New York, 1962), Chap. 4.

²B. Sonntag, in *Rare Gas Solids*, edited by M. L. Klein and J. A. Venables (Academic, New York, 1976), Vol. 2, Chap. 17.

³J. Daniels, *Opt. Commun.* **2**, 352 (1970).

⁴E. Boursey *et al.*, *Phys. Rev. Lett.* **41**, 1516 (1978).

⁵P. Gürtler and E. E. Koch, *Chem. Phys.* **49**, 305 (1978).

⁶A. Skerbele and E. N. Lassette, *J. Chem. Phys.* **53**, 3806 (1970).

⁷N. Oda and T. Osawa, *J. Phys.* **B 14**, L563 (1981).

⁸E. Fainelli, R. Camilloni, G. Petrocelli, and G. Stefani, *Nuovo Cimento* **9D**, 33 (1987).

⁹S. R. Nagel and T. A. Witten, *Phys. Rev. B* **11**, 1623 (1975).

¹⁰H. P. Kelly, *Phys. Rev.* **182**, 84 (1969).

¹¹S. E. Schnatterly, in *Solid State Physics*, edited by H. Ehrenreich, F. Seitz, and D. Turnbull (Academic, New York, 1979), Vol. 34.

¹²P. C. Gibbons, J. J. Ritsko, and S. E. Schnatterly, *Rev. Sci. Instrum.* **46**, 1546 (1975).

¹³C. Tarrío, S. E. Schnatterly, and E. L. Benitez, *Rev. Sci. Instrum.* (to be published).

¹⁴R. Wyckoff, *Crystal Structures* (Wiley, New York, 1963), Vol. 1, p. 129.

¹⁵J. R. Fields, Ph.D. thesis, Princeton University, 1975 (unpublished).

¹⁶P. Livins, T. Aton, and S. E. Schnatterly, *Phys. Rev. B* **38**, 3511 (1988).

¹⁷D. Y. Smith, in *The Handbook of Optical Constants*, edited by E. R. Palik (Academic, Orlando, 1986), Chap. 3.

¹⁸G. R. Alms, A. K. Burnham, and W. D. Flygare, *J. Chem. Phys.* **63**, 3321 (1975).